



## Curie Depth Analysis of the Salton Sea Region, Southern California

KEVIN MICKUS<sup>1</sup> and MUSA HUSSEIN<sup>2</sup>

**Abstract**—Aeromagnetic data were analyzed to determine the bottom of magnetic bodies that might be related to the Curie point depth (CPD) by 2D spectral and 3D inversion methods within the Salton Trough and the surrounding region in southern California. The bottom of the magnetic bodies for 55 × 55 km windows varied in depth between 11 and 23 km in depth using 2D spectral methods. Since the 55 × 55 km square window may include both shallow and deep source, a 3D inversion method was used to provide better resolution of the bottom of the magnetic bodies. The 3D models indicate the depth to the bottom of the magnetic bodies varied between 5 and 23 km. Even though both methods produced similar results, the 3D inversion method produced higher resolution of the CPD depths. The shallowest depths (5–8 km) occur along and west of the Brawley Seismic Zone and the southwestern portion of the Imperial Valley. The source of these shallow CPD values may be related to geothermal systems including hydrothermal circulation and/or partially molten material. Additionally, shallow CPD depths (7–12 km) were found in a northwest-trending zone in the center of the Salton Trough. These depths coincide with previous seismic analyses that indicated a lower crustal low velocity region which is believed to be caused by partially molten material. Lower velocity zones in several regions may be related to fracturing and/or hydrothermal fluids. If the majority of these shallow depths are related to temperature, they are likely associated with the CPD, and the partially molten material extends over a wider zone than previously known. Greater depths within the Salton Trough coincide with the base of basaltic material and/or regions of intense metamorphism intruded by mafic material in the middle/lower crust.

**Key words:** Aeromagnetic anomalies, Curie point depth, heat flow, inversion, spectral methods, salton Trough.

### 1. Introduction

The distribution of temperature variations is important in determining the rheological properties of

the lithosphere that can aid in determining the extent of rifting within a region (CHAPMAN and FURLONG 1992). Although the local temperature distribution is not commonly measured, it may be determined by variations in regional heat flow (POLLACK *et al.* 1993). The heat flow measurements are usually made in bore holes on land that are spaced tens to hundreds of kilometers apart and are not uniformly spaced. Additionally, heat flow measurements may be affected by near-surface and surface temperature variations including groundwater flow and long-term surface temperature variations. To determine the temperature variations in regions where heat flow measurements are absent, geochemical or geophysics methods can be used to indirectly infer the temperature at given depths. Geochemical methods include helium isotope ratios from gases in hot springs (SANO and WAKITA 1985) and silica concentration in hot springs (SWANBERG and MORGAN 1978). Geophysical methods include magnetics, magnetotellurics (MT), and seismic velocity estimates from tomographic studies that can be used to indirectly infer the presence of high heat flow. Magnetotellurics and seismic methods only provide indirect evidence of low electrical resistivity or seismic P- and S-wave velocities that may indicate high heat flow but do not provide estimates of temperatures. However, the magnetic method can be used to estimate the Curie point depth (CPD) by determining the bottom of magnetic sources (e.g., SPECTOR and GRANT 1970; BHATTACHARYYA and LEU 1975; SHUEY *et al.* 1977; BLAKELY 1988; TANAKA *et al.* 1999; ROSS *et al.* 2006; ESPINOSA-CARDENA and CAMPOS-ENRIQUEZ 2008; BOULIGAND *et al.* 2009). The use of the CPD in determining the heat flow is still problematic because the bottom of magnetic source may not reflect temperature, but rather lithologic variations and estimating the bottom depth determined from magnetic interpretation methods can suffer from poor

<sup>1</sup> Department of Geography Geology and Planning, Missouri State University, Springfield, MO 65897, USA. E-mail: kevinmickus@missouristate.edu

<sup>2</sup> Department of Geological Sciences, University of Texas at El Paso, El Paso, TX 79968-0555, USA.

accuracy (TANAKA *et al.* 1999; RAVAT *et al.* 2007). Furthermore, the CPD may depend on composition and the Curie temperature of the magnetic minerals.

The depth to the Curie isothermal point using magnetic data can be accomplished by two different methods. The most popular technique is the spectral method, where the depth is estimated by calculating the spectrum due to either an isolated anomaly using one-dimensional spectral methods (e.g., BHATTACHARYYA and LEU 1975), the two-dimensional (2D) azimuthally averaged spectrum of a region of magnetic data (e.g., SPECTOR and GRANT 1970; SHUEY *et al.* 1977; MAUS and DIMRI 1996; BLAKELY 1988; TANAKA *et al.* 1999), or fractal-based spectral methods (e.g., MAUS *et al.* 1997; BOULIGAND *et al.* 2009). In all cases, the spectra are used to determine the top and bottom of a magnetic source, with the bottom of the source that assumed to be at the CPD. While the spectral methods are widely used, MAUS and DIMRI (1996) have showed that if used improperly, the spectral methods have limited depth information. The other method is to use forward modeling or inversion methods to model isolated magnetic anomalies (BYERLY and STOLT 1977; HONG 1982; MICKUS 1989) or three-dimensional (3D) inversion of a region of magnetic data (HUSSEIN *et al.* 2012) to determine the depth of the magnetic sources. In all these methods, the depth to the bottom of the source is assumed to be at the Curie temperature of magnetic minerals (for instance magnetite is 580 °C). However, neither spectral nor modeling methods work with complete reliability and the estimated depths must be assessed using outside constraints from other geological and geophysical investigations (RAVAT *et al.* 2007).

In the present study, we applied the 2D power density spectral method and 3D inversion of aeromagnetic anomalies within and surrounding the Salton Trough region of California to determine the depth of the bottom of magnetic sources.

The Salton Trough region is complex tectonic region that is the product of late Cenozoic deformation related to the evolution of the Pacific and North American plate boundary in southern California (ATWATER 1970; AXEN *et al.* 2000; DORSEY *et al.* 2007; STEELY *et al.* 2009). Specifically, the Salton Trough is a large transtensional basin that lies along the oblique-divergent plate boundary in southern

California that contains up to 10–12 km of nonmarine sediments (DORSEY *et al.* 2007). The transtensional tectonic regime is associated with high heat flow values that peak at the southern end of the Salton Sea and regions within the Imperial Valley (LACHENBRUCH *et al.* 1985) (Triangles in Fig. 3). Regional geophysical studies have indicated the presence of thinned crust and the possibility of partially molten material under the Salton Trough (ELDERS *et al.* 1972; FUIS *et al.* 1984; HUSSEIN *et al.* 2011). To determine the extent of the regional high heat flow values and the relationship to the tectonic evolution of the Salton Trough, a magnetic analysis in the form of spectral and 3D inverse methods was undertaken.

## 2. Tectonic and Geophysical Setting

The present day configuration of the North American-Pacific plate boundary in the Gulf of California and Salton Trough region started approximately 6 Ma (OSKIN *et al.* 2001). In the Salton Trough region, the San Andreas, San Jacinto, and Elsinore accommodate approximately 80 % of the of the 50–55 mm/year plate motion between the Pacific and North American plates (DEMETS and DIXON 1999; Fig. 1). Using traditional geological methods (e.g., geomorphology, trenching), the amount of slip along the San Andreas Fault was found to be twice that along the San Jacinto Fault (LINDSEY *et al.* 2013). The slip rate found along the Elsinore Fault was considerably less than the other two faults (FIALKO 2006; FAY and HUMPHREYS 2005). The San Jacinto Fault is more seismically active and structurally complex than the other two faults because it consists of a complex zone of overlapping strike-slip segments (SANDERS and MAGISTRALE 1997; WESNOUSKY 1986).

The Salton Trough subsided from the late Miocene to early Pleistocene due to regional extension and transtension (AXEN and FLETCHER 1998; DORSEY 2010; DORSEY and UMHOEFER 2012). The present day Salton Trough differs from analogous structures to the south in the Gulf of California primarily because of the large volumes of sediment deposited through the growth of the Colorado River delta during the past 5 million years which may have played a strong role in reducing the apparent structural relief in the

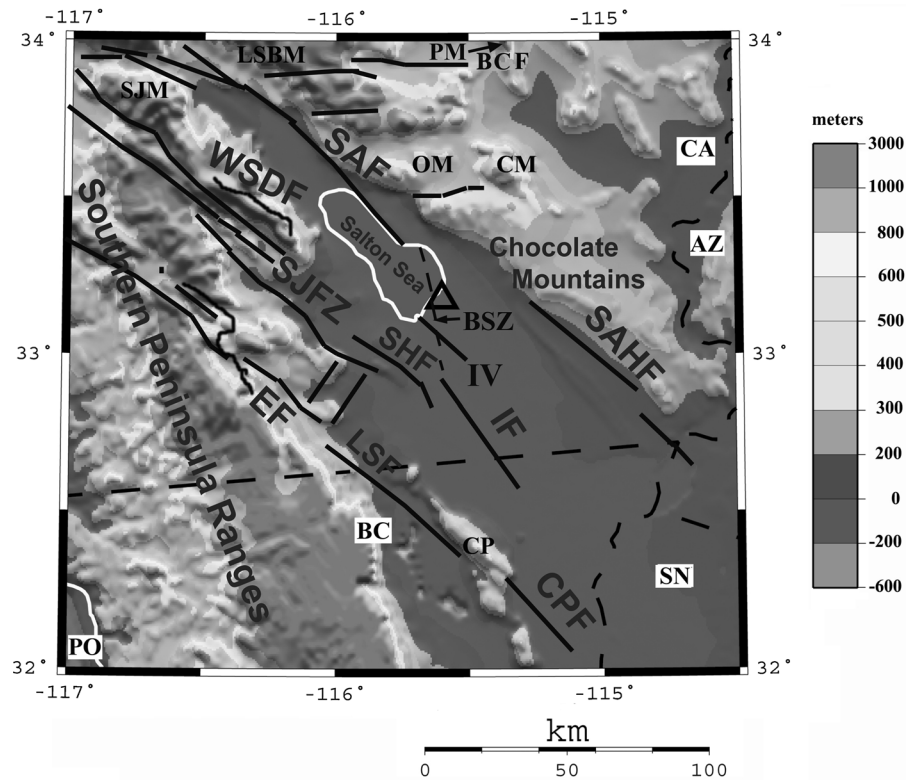


Figure 1

General location map of the Salton Trough and surrounding regions in southern California showing topography and major faults (*bold lines*). The major faults include Blue Cut Fault (BCF), Brawley Seismic Zone (BSZ), Cerro Prieto Fault (CPF), Elsinore Fault (EF), Imperial Fault (IF), Imperial Valley (IV), Laguna Salada Fault (LSF), San Andreas (SAF), Sands Hill Fault (SAHF), San Jacinto Fault Zone (SJFZ), Superstition Hills Fault (SHF), Western Salton Detachment Fault (WSDF). Mountain ranges include San Jacinto (SJM), Orocoopia (OM), Chuckwalla (CM), Little San Bernardino (LSBM), Pinto (PM). *Triangle* shows the location of the Salton Sea geothermal field. AZ Arizona, CA California, BC Baja California, CP Cerro Prieto, SN Sonora, PO Pacific Ocean, SS Salton Sea

Salton Trough (PARSONS and McCARTHY 1996; DORSEY *et al.* 2007). Seismic reflection/refraction and gravity studies have indicated that the total thickness of the sediment in the Salton Trough varies between 5 and 12 km (ELDERS *et al.* 1972; FUIS *et al.* 1984; HUSSEIN *et al.* 2011). This large volume of sediment, especially the felsic material deposited by the Colorado River, has been metamorphosed by the active magmatism and high heat flow values (FUIS *et al.* 1984; DORSEY 2010).

The Salton Trough is a region with high heat flow, Quaternary rhyolitic volcanism, abundant and shallow seismicity, geothermal energy production, and continued subsidence (ELDERS *et al.* 1972; DOSER and KANAMORI 1986; SASS *et al.* 1988; HERZIG and JACOBS 1994; SCHMITT and VAZQUEZ 2006). The above characteristics have been investigated by a large number

of geophysical surveys including seismic reflection/refraction, gravity, and heat flow (e.g., BIEHLER 1964; ELDERS *et al.* 1972; FUIS *et al.* 1984; LACHENBRUCH *et al.* 1985; SASS *et al.* 1988; PARSONS and McCARTHY 1996; BROTHERS *et al.* 2009; HUSSEIN *et al.* 2011). Seismic reflection/refraction and gravity modeling showed that the crust is thin (21–22 km) beneath the Salton Trough with thicker crust (27–28 km) beneath the Chocolate Mountains and Eastern Peninsula Ranges (FUIS *et al.* 1984; PARSONS and McCARTHY 1996; HAN *et al.* 2013a, b).

The recent Salton Seismic Imaging Project (SSIP) (HAN *et al.* 2013a, b) which consisted of a detailed seismic refraction/reflection profile along the central portion of the Salton Trough showed that the crustal thickness varied between 17 and 18 km and that the crystalline basement has higher velocities beneath the

Salton Sea geothermal region. This high velocity is possibly related to either to metamorphism, hydrothermal mineralization, or magmatism. The seismic refraction/reflection results were supported by broadband seismic studies (tomography, receiver functions, ambient noise analyses) (ZHU and KANAMORI 2000; BARAK *et al.* 2011; HUSSEIN *et al.* 2011; ALLAM and BEN-ZION 2012) where the dip on the crust/mantle boundary is highest within the Eastern Peninsula Ranges (LEWIS *et al.* 2000). Additionally, the middle to lower crust beneath the Salton Trough has higher velocities and densities than the surrounding region and have been interpreted to be oceanic crust (FUIS *et al.* 1984). The detailed broadband seismic analysis by BARAK *et al.* (2011) and KINSELLA *et al.* (2012) showed that the Moho thinned beneath the Salton Trough and the upper mantle consists of low velocity material. Receiver function and Rayleigh-wave tomographic analyses have shown that the upper mantle beneath the Salton Trough has lower velocities possibly caused by asthenospheric upwelling of partially molten material (ZHU and KANAMORI 2000; YANG and FORSYTH 2008).

### 3. Aeromagnetic Data

Aeromagnetic data were compiled from surveys over the study area that had different parameters including line spacings, flight elevations, and the year of data collection (BANKEY *et al.* 2002). The data from each individual survey were reprocessed for diurnal variations, flight heading, and errors in flight elevation. The data had the Definitive Geomagnetic Reference Field removed for the date of the original survey. Then the individual surveys were merged and regridded into regional compilations (BANKEY *et al.* 2002). The regional grids were resampled into a grid with a spacing of 1 km, and the original grids were either downward or upward continued to a constant 0.305 km above the Earth's surface. Finally, the regional grids were merged together to produce a final grid of North America. However, this grid had spurious long wavelength anomalies that were caused by merging the multiple surveys, so the final grid had wavelengths greater than 500 km removed. More details about the merging of the individual surveys

can be found in BANKEY *et al.* (2002). The aeromagnetic data for Salton Trough and the surrounding region were gridded at 1.0 km spacing and contoured at 50 gammas to produce a magnetic anomaly map (Fig. 2).

Magnetic anomalies usually reflect lateral variations in magnetic mineralogy (which mostly consists of magnetite) of the rocks from crustal to mid to lower crustal depths depending on the heat flow in the region. Shorter wavelength anomalies can commonly be correlated to surface or near-surface geology; however, longer wavelength anomalies may be caused by either deep magnetic mineralogy variations or variations in the CDP caused by regional heat flow differences. Within the Salton Trough region, the magnetic anomalies generally reflect the magnetic susceptibility variations within the Proterozoic basement rock types, Mesozoic intrusions, and Cenozoic volcanic rocks (GRISCOM and MUFFLER 1971; LANGENHEIM and JACHENS 2003; LANGENHEIM *et al.* 2004, 2005, LANGENHEIM and POWELL 2009). The Salton Trough is mainly characterized by a smooth magnetic anomaly pattern (anomaly 1, Fig. 2) that is caused mostly by the thick sedimentary section (FUIS *et al.* 1984; PARSONS and MCCARTHY 1996) that attenuates the magnetic signature of the rock types beneath the Salton Trough (Fig. 2). Given the high heat flow within the Salton Trough (LACHENBRUCH *et al.* 1985), the magnetic signature of the rock unit may be lower due to possible shallow Curie isothermal depths. Superimposed on the smooth magnetic pattern are several short wavelength magnetic maxima (anomaly 2, Fig. 2) that may be due to magnetic material associated with volcanic material (GRISCOM and MUFFLER 1971). Northwest of the Salton Sea the magnetic anomalies are caused by a pluton in the upper part of the Eastern Peninsular Ranges mylonite zone (LANGENHEIM *et al.* 2004). A conspicuous magnetic anomaly occurs over the Salton Sea geothermal anomaly (Fig. 2) and five rhyolitic domes at the southern end of the Salton Sea and over the Cerro Prieto geothermal field (Fig. 1) in northern Baja California. The southern Salton Sea magnetic anomaly is thought to be associated with igneous intrusive material buried at approximately 2 km in depth and extends at least 30 km to the northwest (GRISCOM and MUFFLER 1971). It is also coincident



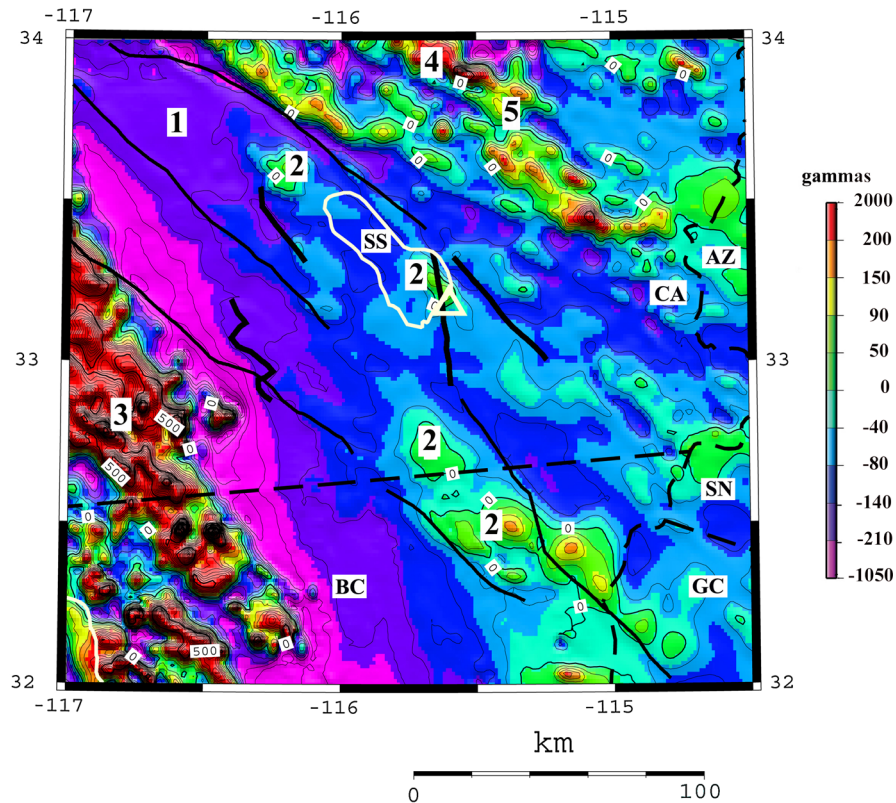


Figure 2

Reduced to the pole magnetic map using an inclination of  $58^\circ$  and declination of  $13^\circ$  of the Salton Trough and surrounding regions. *Bold numbers* represent anomalies discussed in the text. *Bold black lines* represent major known faults. The *white triangle* and *white square* are the locations of the Salton Sea and Cerro Prieto geothermal fields, respectively. Contour interval is 50 gammas. AZ Arizona, CA California, BC Baja California, SN Sonora, SS Salton Sea

with a large amplitude gravity maximum which argues for a mafic source rather than a granitic source. The magnetic maximum at the Cerro Prieto geothermal anomaly occurs over rhyodacitic volcanic domes that contain numerous diabase sills (DE BOER 1980; GOLDSTEIN *et al.* 1984) with the source of the magnetic anomaly being a body that extends to 6 km beneath the surface (GOLDSTEIN *et al.* 1984; ESPINOSA-CARDENA and CAMPOS-ENRIQUEZ 2008).

Besides the magnetic anomalies occurring with the known geothermal anomalies, there are other magnetic maximum (anomalies 2, Fig. 2) within the Salton Trough. These anomalies are not associated with known magnetic rock types considering their size and amplitude that they may be caused by igneous material beneath the Cenozoic sediments within the Salton Trough or the source could reside in the crystalline basement. There are scattered volcanic

rocks cropping out southwest of Cerro Prieto (MORAN-ZENTENO *et al.* 1994) which supports this interpretation.

Even though the magnetic field over the Salton Trough is relatively smooth with several short wavelength maxima, a closer look at the data indicates that there are regions with low amplitude maxima and minima. Even though not obvious in Fig. 2, a residual magnetic anomaly map constructed by band-passing wavelengths between 10 and 75 km indicates several low amplitude anomalies (anomalies 1–4, Fig. 3) within the Salton Trough. Anomalies 2 and 4 reflect thicker sediments as imaged by seismic refraction surveys (FUIS *et al.* 1984; KOHLER and FUIS 1986; PARSONS and MCCARTHY 1996), an ambient noise analysis from broadband seismic stations (KINSELLA *et al.* 2012), and integrated geophysical study (HUSSEIN *et al.* 2011). Anomaly 3 has been

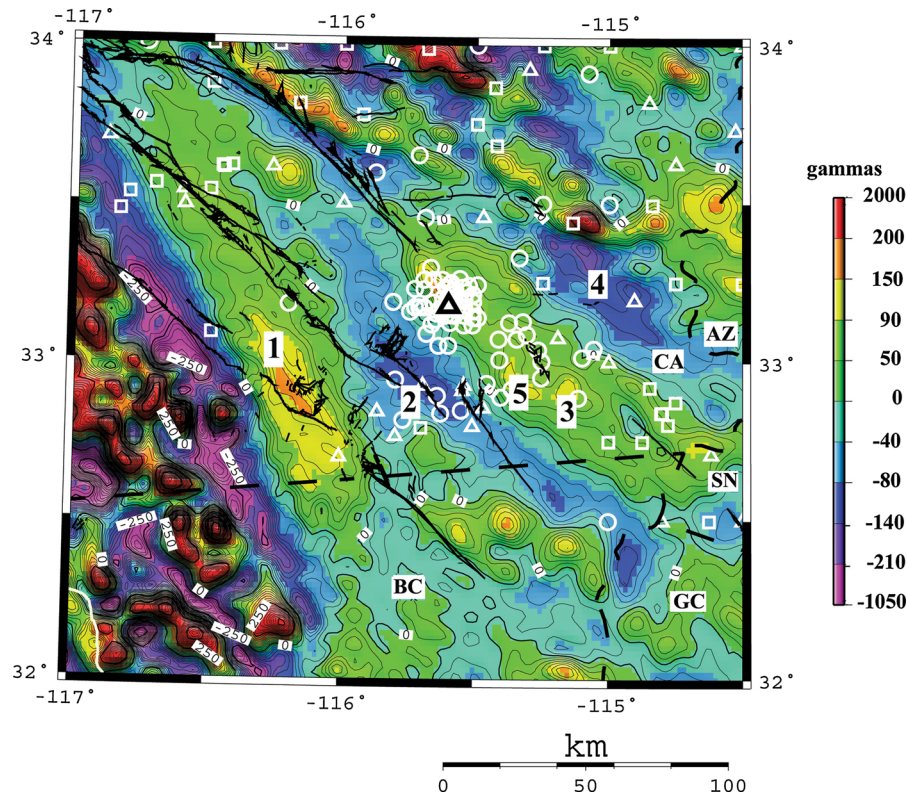


Figure 3

Regional magnetic anomaly map of the Salton Trough and surrounding regions created by passing wavelengths between 10 and 75 km. **Bold black lines** represent major known faults. **Black triangle** is the location of the Salton Sea geothermal plant. **White squares** represent heat flow measurements less than  $70 \text{ mW/m}^2$ , **white triangles** represent heat flow measurements between  $70$  and  $100 \text{ mW/m}^2$ , and **white circles** represent heat flow measurements greater than  $100 \text{ mW/m}^2$  (BLACKWELL and RICHARDS 2004). Contour interval is 50 gammas. AZ Arizona, CA California, BC Baja California, SN Sonora, PO Pacific Ocean, SS Salton Sea

modeled as a dense mafic intrusion by seismic refraction, gravity, and a seismic ambient noise analysis (FUIS *et al.* 1984; PARSONS and MCCARTHY 1996; BARAK *et al.* 2011; KINSELLA *et al.* 2012). SSIP results have shown that the highest basement velocities occur to the west of anomaly 3 and anomaly 5 (Fig. 3; HAN *et al.* 2013a, b). These high velocities were been interpreted to be either magmatic material, intense metamorphism or hydrothermal mineralization (HAN *et al.* 2013a, b). Anomaly 3 is also associated with a gravity maximum (FUIS *et al.* 1984), and gravity modeling has indicated that the top is between 12 and 15 km (PARSONS and MCCARTHY 1996). However, a seismic ambient noise analysis indicates that the top may be at 9 km (BARAK *et al.* 2011), and the SSIP models indicate a shallower (2–4 km) source for the high-density/velocity basement lithologies. The seismic ambient noise analysis

indicated that the deeper high-density body (mafic?) associated with anomaly 3 (Fig. 3) extends nearly to the California/Baja California border nevertheless the lack of stations near the border limited the resolution of their results. However, from the residual magnetic anomaly map (Fig. 3), the mafic body may extend at least 25 km south of the Baja California border. The source of anomaly 1 (Fig. 3) is more problematic but could be an extension of either the dense, deeper mafic material, or the shallower high velocity material imaged under the Brawley Seismic Zone (HAN *et al.* 2013a, b). If anomaly 1 (Fig. 3) is caused by a mafic body, it may be relatively thin so that the seismic noise analysis did not image the body.

Outside the Salton Trough, the magnetic field mainly reflects the magnetic properties of the basement rocks (GRISCOM and JACHENS 1990; MICKUS and JAMES 1991; LANGENHEIM *et al.* 2005; LANGENHEIM and

POWELL 2009). The western Peninsula Ranges (Fig. 1) consist of a series of magnetic maxima (anomaly 3, Fig. 2), which extends to the southern end of the Baja Peninsula, that is probably associated with mafic lithologies within the mainly Jurassic–Cretaceous arc rocks and older oceanic rocks (LANGENHEIM and JACHENS 2003). Even though Cenozoic volcanic rocks are exposed in the southern Peninsula Range, they are thin and have a highly variable magnetic susceptibility which makes them unlikely to produce such high amplitude magnetic anomalies (LANGENHEIM and JACHENS 2003; LANGENHEIM *et al.* 2005). These high amplitude magnetic anomalies are in contrast to the region northeast of the San Andreas Fault where the magnetic anomalies consist of a series of short wavelength magnetic maxima and minima of smaller amplitudes (Fig. 2). These magnetic maxima in general coincide with Precambrian metamorphic and igneous rocks and Mesozoic igneous rocks (MICKUS and JAMES 1991; LANGENHEIM and POWELL 2009). The higher amplitude magnetic anomalies occur over the Jurassic intrusive rocks (Pinto Mountains, anomaly 4, Fig. 2) rather than the Cretaceous intrusive bodies (Coxcomb Mountains, anomaly 5, Fig. 2; LANGENHEIM and POWELL 2009).

One problem with using aeromagnetic data in determining the CPD is that any given magnetic anomaly may be caused by either increasing temperature that causes the magnetization of the mineral to disappear or by the lack of magnetic minerals at a certain depth (ROSS *et al.* 2006). Without detailed heat flow data and/or drilling information, this determination may be difficult. Within the Salton Trough, the majority of the wells with heat flow measurements are within the Salton Sea geothermal area (Fig. 3). Even though there are heat flow values in the Salton Trough (LACHENBRUCH *et al.* 1985; NEWMARK *et al.* 1988; SASS *et al.* 1994), the detailed thermal structure is only known in general terms. To use magnetic data to determine the CPD, there must be deep crustal magnetic sources. HUSSEIN *et al.* (2012) constructed a regional magnetic anomaly map by subtracting an upward continued magnetic field from the total field magnetic field to show that the majority of magnetic sources are deep. In this study, we used the pseudogravity transformation (BARANOV 1957) to

emphasize the more voluminous magnetic sources (LANGENHEIM *et al.* 2004). The pseudogravity transformation converts the magnetic field into an equivalent gravity field where all the magnetic minerals are replaced by dense material. This transformation emphasizes the longer wavelength magnetic anomalies most likely caused by voluminous and perhaps deeper sources (LANGENHEIM *et al.* 2004). The pseudogravity transformation map (Fig. 4) indicates that the Salton Trough contains a relatively smooth magnetic potential field. Still, there are several maxima (anomalies 1–5, Fig. 4) that are related to deeper sources.

#### 4. Curie Point Depth Analysis

##### 4.1. Spectral Analysis

Spectral methods have routinely been used in the analysis of magnetic data to determine the CPD by analyzing magnetic data over large regions (e.g., SHUEY *et al.* 1977; BLAKELY 1988; ROSS *et al.* 2006). The main problem with these methods is that small-scale variations in the CPDs are difficult to determine because the determination of the depth to the bottom of a magnetic source is a function of the region analyzed (BOULIGAND *et al.* 2009; HUSSEIN *et al.* 2012). In general, the width of the area analyzed must be at least three to four times the actual depth to the bottom of a magnetic source in order to be confident of the determined depth.

In order to determine the spectrally determined depth, the method of TANAKA *et al.* (1999) and MANEA and MANEA (2011) which was in turn based on the technique of BHATTACHARYYA and LEU (1975) and OKUBO *et al.* (1985) was used to estimate the bottom of magnetic sources. TANAKA *et al.* (1999) showed that by determining the radially averaged power density spectra of the magnetic anomalies over a region, one could estimate the depth to the bottom of a magnetic source. To determine the top of a magnetic source, the radially averaged power density spectra  $[\ln(\Phi_{\Delta T}(kl)^{1/2})]$  are plotted, and a straight line is fit through the lower wavenumber portions (0.03–0.2 rad/km) of the curve. The depth to the centroid of a magnetic source is determined in a similar fashion; however, the quantity



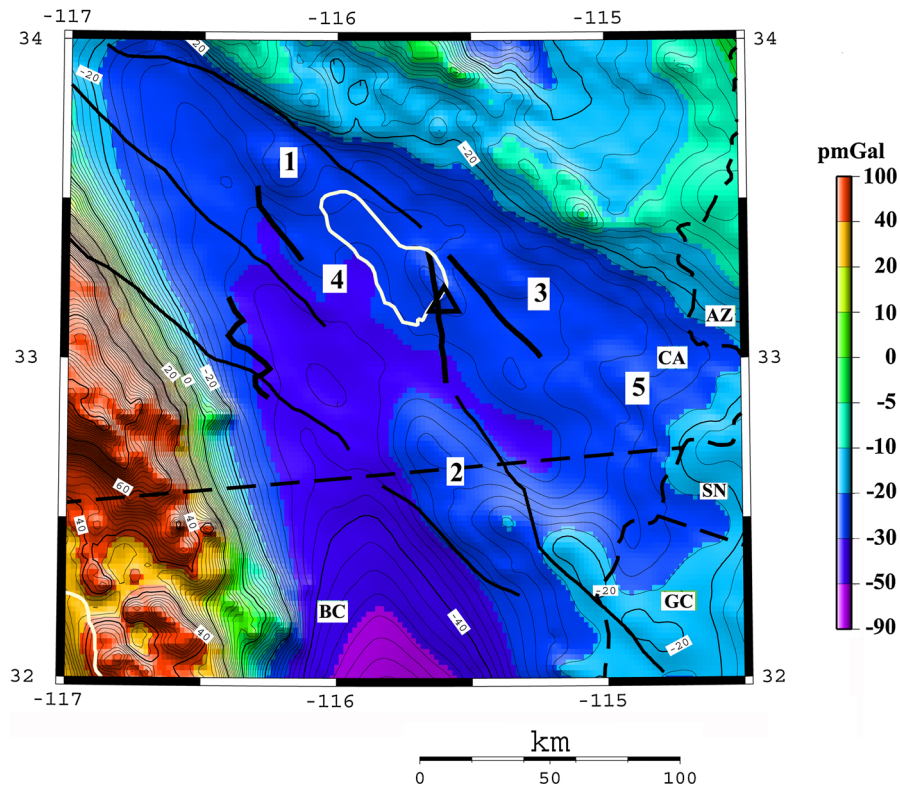


Figure 4

Pseudogravity anomaly map of the Salton Trough and surrounding regions. **Bold black lines** represent major known faults. **Bold numbers** represent anomalies discussed in the text. **Black triangle** is the location of the Salton Sea geothermal plant. Contour interval is 2 mGal

$[\ln(\Phi_{\Delta T}(kl)^{1/2})/kl]$  is plotted, and a straight line is fit through the higher wave numbers (0.5–0.8 rad/km). The basal depth of the magnetic source is then calculated from  $Z_b = 2Z_0 - Z_t$ , where  $Z_t$  is the top bound and  $Z_0$  is the centroid.

Since we are trying to map CPD's of relatively small features (e.g., geothermal areas within the Salton Trough), small windows are needed to estimate the radially averaged power spectra. A previous study that included the Salton Trough (BOULIGAND *et al.* 2009) used a  $100 \times 100$  km window to show that the CPDs ranged from 13 to 17 km. BOULIGAND *et al.* (2009) showed that large window sizes are needed to recover low wavenumbers in the radial power spectrum that represent the depth to the bottom of magnetic sources. However, a  $100 \times 100$  km window is too large to reliably image small-scale CPD variations (RAVAT *et al.* 2007) as the higher wavenumbers are needed to image the shallower depths. To estimate the depths to the shallower

magnetic sources, we tried a variety of window sizes from  $20 \times 20$  to  $100 \times 100$  km and found that a  $55 \times 55$  km window best delineated CPD depths between 5 and 20 km. Additionally, we overlapped our analysis regions by 10 km on each side in order to minimize the well-known edge effects of using the Fast Fourier Transform.

Two examples of the power spectrum analysis from two different regions within the Salton Trough are shown in Figs. 5 and 6. One problem with using the spectral methods is determining what wavenumbers to use to measure the slope as slight variations in the location of the slope can lead to different depths (RAVAT *et al.* 2007). To determine the variations in the depths to the bottom of magnetic sources, we measured the wavenumber slopes at three different locations for both the top and centroid of the magnetic source. The variability for the top of the magnetic source was between 0.1 and 0.3 km, while the variability in depth values for the centroid of the

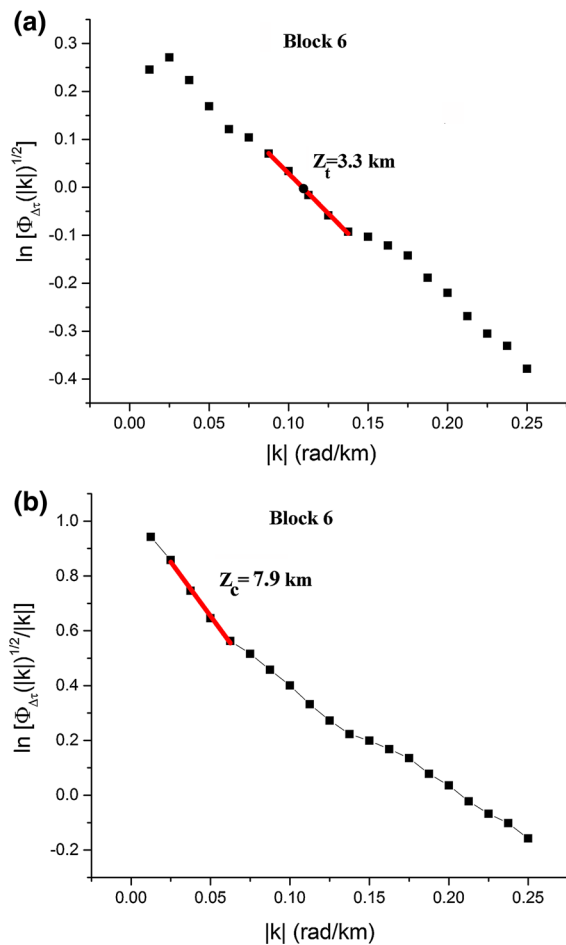


Figure 5

Spectra for **a**: for the top of the magnetic source and **b**: for the centroid of magnetic source of block 6 (Fig. 7). The *bolded straight lines* in **a** and **b** represent the slopes used to determine the top and centroid of the magnetic source. These values were then used to estimate the Curie isothermal depth.  $Z_t$  represents the top of the magnetic source and  $Z_c$  represents the centroid of the magnetic source

magnetic source was between 0.7 and 1.3 km. The above range in depth values would lead to errors between 0.8 and 2.3 km in the CPDs.

Figure 7 shows the results of the power spectrum analysis to determine the bottom of the magnetic sources. The estimated depths range from 11.2 for block 20–23 km for block 3. These numbers roughly agree with the results of BOULIGAND *et al.* (2009) who concluded using a larger window that the Salton Trough had CPD depths between 12 and 14 km with shallow values ( $<10$  km) in the Mojave region northeast of the Salton Trough. Two regions of

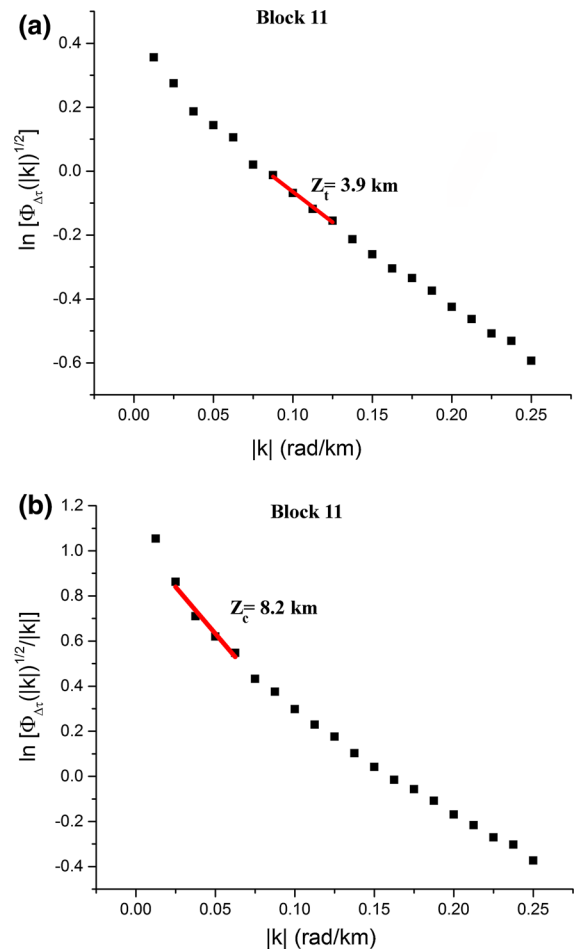


Figure 6

Spectra for **a**: for the top of the magnetic source and **b**: for the centroid of magnetic source of block 11 (Fig. 7). The *bolded straight lines* in **a** and **b** represent the slopes used to determine the top and centroid of the magnetic source. These values were then used to estimate the Curie isothermal depth.  $Z_t$  represents the top of the magnetic source and  $Z_c$  represents the centroid of the magnetic source

particular interest include blocks 10 and 16 where the known geothermal fields (Salton Sea and Cerro Prieto) exist. The high heat flow values ( $>1000$  mW m $^{-2}$ ) in these geothermal fields (SASS *et al.* 1994) suggest that the CPD should be shallower than the power spectrum analysis determined values of 16.4 and 14.8 km, respectively. These depths show the limitation of the power spectrum method in determining CPD values of spatially small anomalies. Of particular interest are the shallower depths in blocks 6, 11, 16, and 20. The shallow values in block 11 can be associated with the low seismic velocities found in the



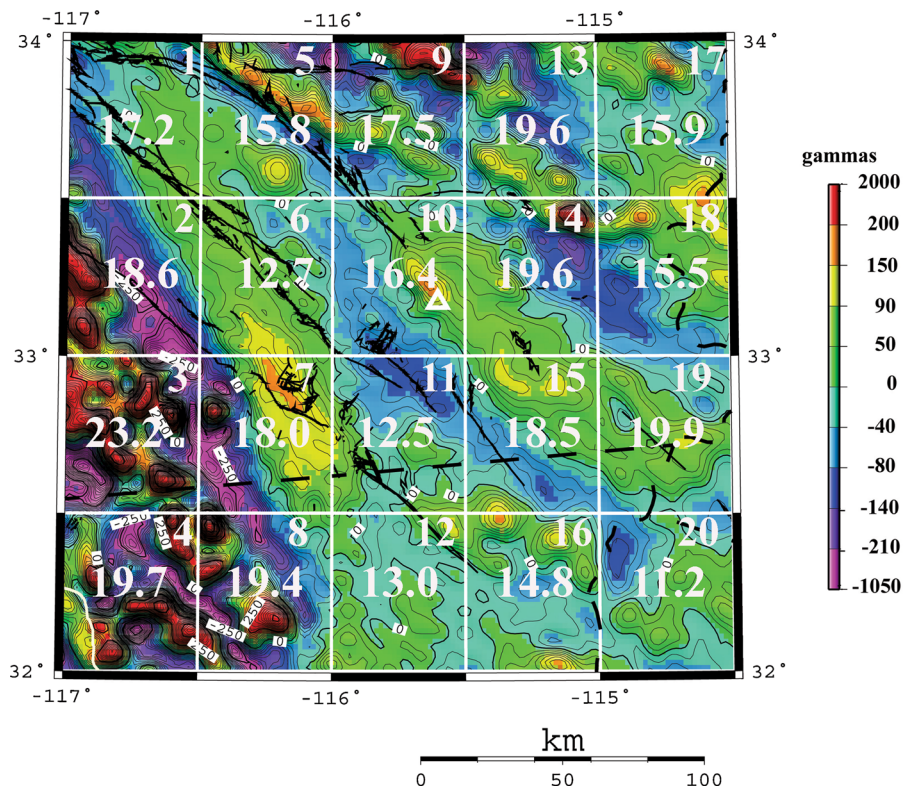


Figure 7

Regional magnetic anomaly map of the Salton Trough and surrounding regions. The *white grid* represents the block in which the spectral analysis was performed to determine the bottom of magnetic source. The *smaller white number* in the upper right corner of each *box* represents the block number and the *larger white number* near the center of each *box* represents the spectrally determined Curie isothermal depth in kilometers. *Bold black lines* represent major known faults. *White triangle* is the location of the Salton Sea geothermal field. Contour interval is 50 gammas

lower crust by seismic ambient noise analyses (KINSELLA *et al.* 2012). Part of the low seismic velocities is attributed to fracturing in the basement or hydrothermal fluids in the northwest portion of block 11, and this low velocities continue into block 10 (HAN *et al.* 2013a, b). If the shallower CPD values are associated with hydrothermal fluids related to magmatic activity, the shallow CPD values to the northwest and southeast of block 11 may represent the extension of these low velocity regions. Additionally, the deeper CPD values in blocks 7 and 15 can be explained by the mafic underplating at 15–20 km in depth imaged by the above seismic studies.

#### 4.2. Three-Dimensional Inversion

The second method of determining the CPD is to model magnetic anomalies due to isolated magnetic

anomalies or a region that contains several magnetic anomalies using forward or inverse methods. The most commonly used approach has been to model isolated anomalies using vertical prisms (BHATTACHARYYA and LEU 1975; SHUEY *et al.* 1977) bodies with a rectangular or cylindrical shape (BYERLY and STOLT 1977) or arbitrarily shaped two- and two-and-one-half-dimensional bodies (HONG 1982; MICKUS 1989). Recently, HUSSEIN *et al.* (2012) determined the depth to the bottom of magnetic sources of a region containing numerous magnetic anomalies using 3D inversion methods. One problem with the above methods except the 3D inversion method is that they model an anomaly due to an isolated body that requires trying to perform a residual anomaly separation. This procedure usually introduces some sort of error in determining the true anomaly related to a body.

The advantages of using 3D inversion are that one does not have to isolate positive magnetic anomalies or determine if the anomaly is over thick volcanic, plutonic, or metamorphic rocks that has to be done in the methods by HONG (1982) and MICKUS (1989). However, one has to interpret the given depths to determine if they truly represent the CPD or just the depth to the bottom of the magnetic mineralogy. In some regions, there may not be enough suitable anomalies to accurately determine regional CPD variations. Within the Salton Trough and the surrounding area, the residual magnetic anomaly map (Fig. 3) and the pseudogravity anomaly map (Fig. 4) indicate that there are several short wavelength, low amplitude anomalies that should be suitable for determining the depths to their source.

To estimate the depth and geometry of the sources of the various anomalies observed in Figs. 2 and 3, a 3D inversion of the reduced to the pole magnetic data was performed using a routine by LI and OLDENBURG (1996). To obtain reliable solution without outside constraints, different inversion parameters (e.g., weighting of the data, data errors, choice of objective function, starting model, and size of model mesh) were considered and varied to test the consistency of our models with the geology. Incorrect choices of these parameters could lead to results that have no relationship to the actual geology despite a low RMS error (LI and OLDENBURG 1996).

The 3D inversion of potential field data requires a large amount of computer memory and thus time if a large number of body cells and data points are used. Since we are trying to model a large area, we modeled the central portion of the Salton Trough including blocks 6, 7, 10, 11, 14, 15, 18, and 19 (Fig. 7). For each model, the minimum-sized cell block is 400 m which gradually increases toward the north-south and east-west edges and toward the bottom of the model. The depth of the blocks was set at 40 km. We tried a variety of starting models (magnetic susceptibilities), and variations in the above inversion parameters in order to determine which features in the model produced by the inversion process were consistently determined. To show the final results, various slices were made (Figs. 8, 9) to illustrate the main features of the models. As with potential field methods, the resolution of the

boundaries decreases with depth, so depth weighting is necessary in order to avoid having the bodies being concentrated near the surface (LI and OLDENBURG 1996). To test the resolution of our models, we inverted the data using different starting models with and without depth weighting. For each model, we ran ten inversion models and determined the depth to the bottom of the magnetic sources under the Salton Sea geothermal area and the Chocolate Mountains. Under the Salton Sea geothermal area, the depth varied by 1.0 km, while it varied by 2.3 km under the Chocolate Mountains.

Figures 8 and 9 indicate that the depth to the bottom of magnetic sources range from 5 to 6 km to approximately 23 km. There is considerable uncertainty in determining the cut off depth, but in general, the depths were chosen at the bottom of the higher magnetic susceptibility values (orange on Figs. 8 and 9). In general, the deeper magnetic sources were found on the eastern edge of the study area (Fig. 10) under the Precambrian metamorphic and Mesozoic granitic rocks within the Chocolate Mountains (JENNINGS 1977). The shallowest depths are along the eastern edge of the eastern Peninsula Range where there are numerous short wavelength magnetic maxima. Within the Salton Trough, the depths to the bottom of the magnetic sources varied widely (7–19 km) with the deeper values occurring southeast of the Salton Sea geothermal area which contains, based on seismic studies (e.g., PARSONS and MCCARTHY 1996; BARAK *et al.* 2011; HAN *et al.* 2013a, b) a high velocity layer (mafic?).

## 5. Discussion

Curie point depth analyses can be used to estimate the thermal and/or geologic structure of a region. Our analysis of the CPD within the Salton Trough and the surrounding region was attempted using power density spectrum methods and inverting magnetic data for 3D magnetic susceptibility distributions. The power density spectrum method roughly estimated the CPDs but probably overestimated these depths in a number of regions including blocks 6, 10, and 12 (Fig. 7) as compared to the CPD's determined from the 3D inversion (Fig. 10). The problem with the power density

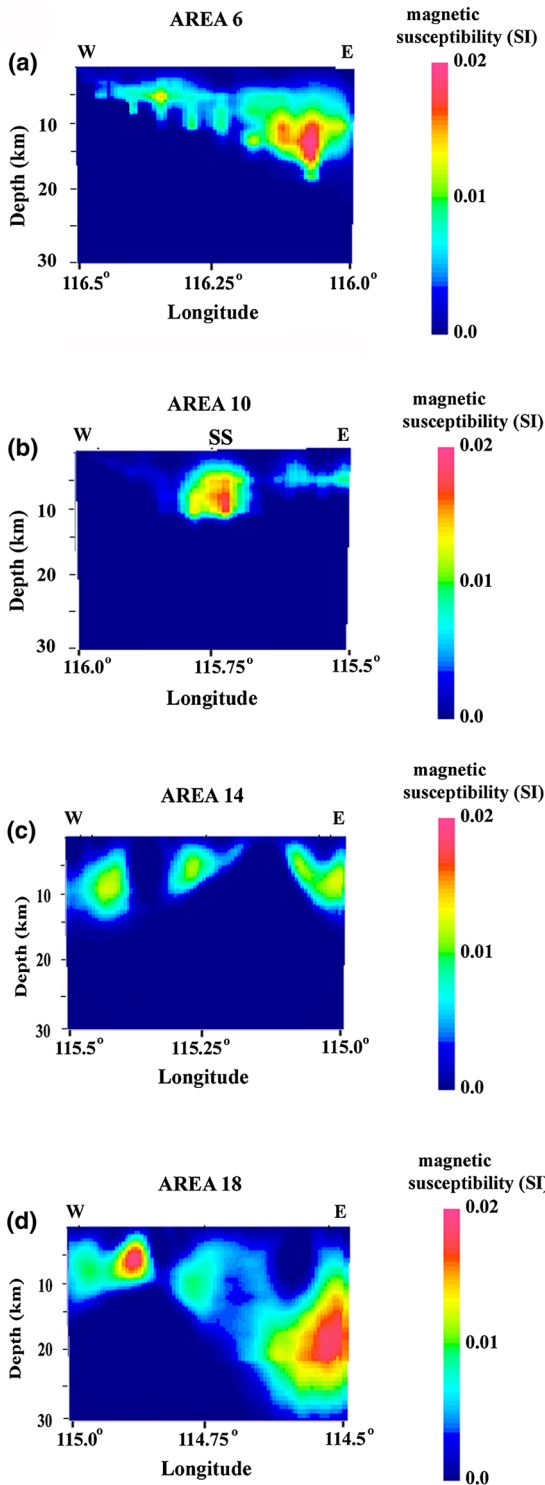


Figure 8

East-west slices of the 3D model inversion models through the center of blocks 6 (a), 10 (b), 14 (c), and 18 (d) (Fig. 7). Block 10 goes through the Salton Sea geothermal field

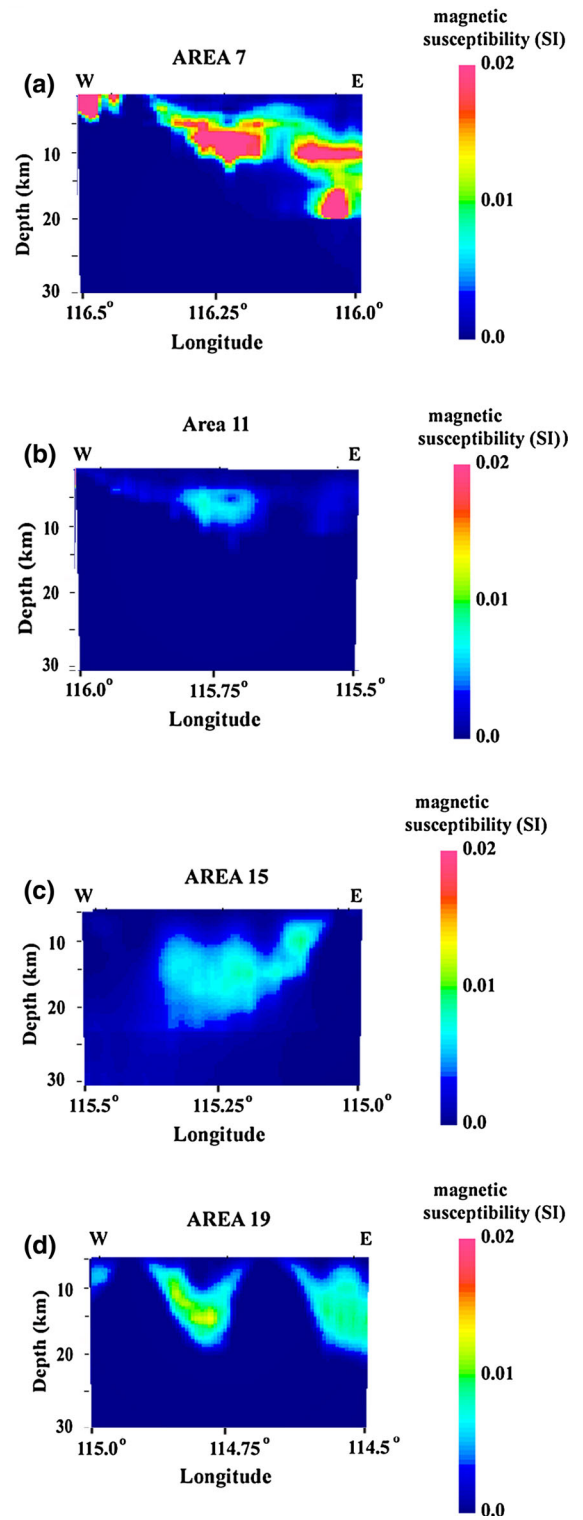


Figure 9

East-west slices of the 3D model inversion models through the center of blocks 7 (a), 11 (b), 15 (c), and 19 (d) (Fig. 7)

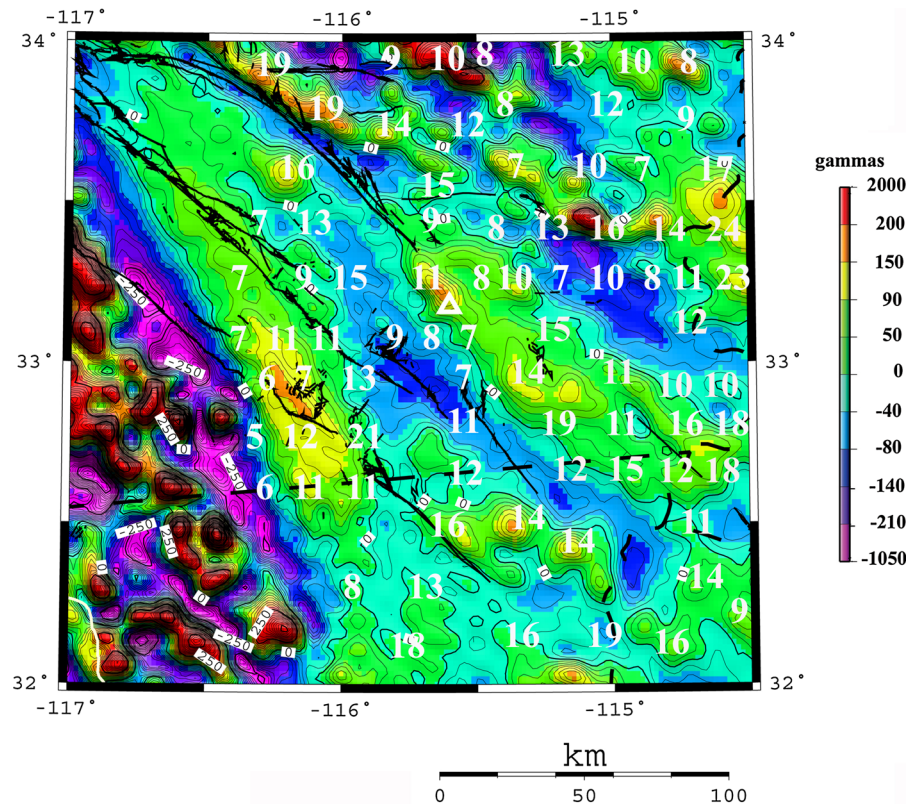


Figure 10

Regional magnetic anomaly map of the Salton Trough and surrounding regions showing the Curie isothermal depth points as determined from the 3D inversion of the magnetic data. All depths are in kilometers. **Bold black lines** represent major known faults. **White triangle** is the location of the Salton Sea geothermal field. Contour interval is 50 gammas

spectrum methods is that they cannot separate the depths to the top and bottom of magnetic sources unless the region analyzed is much larger (3–4 times) than the maximum depth to the bottom of a body (Blakely, personal communication, 2012) and thus cannot image small-scale variations within the CPDs. This limitation has been noted by other authors (e.g., TANAKA *et al.* 1999; BOULIGAND *et al.* 2009) and is obvious in blocks 6 and 7 where the inversion imaged several regions with shallow CPDs (7–8 km), while the power spectrum results were greater than 12 km. Given the complex magnetic anomaly pattern within the Eastern Peninsula Ranges where anomalies were modeled with both shallow (<10 km) and deep (>10 km) (LANGENHEIM and JACHENS 2003), such a result is not surprising. However, the power spectrum analysis did produce results that roughly agreed with the results of BOULIGAND *et al.* (2009) who found that within the Salton Trough the CPDs varied between 12

and 14 km. Our results produced more variation to the CPD with several regions (e.g., blocks 10, 14, and 15) producing deeper values (Fig. 7). This is probably because of our smaller analysis windows imaged laterally smaller CPD variations.

The 3D inversion models (Figs. 8, 9) provided more spatially detailed depths to the bottom of the magnetic sources than the power spectrum method. Assuming that most of these depths represent the Curie isothermal point, the CPDs are shown in Fig. 10. The depths were selected by determining the maximum depths shown in the bodies in Figs. 8 and 9, which are east–west slices in the middle of the 3D model. The other depths were chosen at east–west slices at distances one quarter and three quarters from the southern edge of each block.

The estimate of heat flow from CPD analyses is dependent on the temperature used for the most



common magnetic mineral, magnetite. The most commonly used value is 580 °C (HAGGERTY 1978). To estimate the heat flow from CPDs, we used the one-dimensional conductive heat flow equation where the temperature gradient is constant. In such an active rifting environment as the Salton Trough, convective heat flow may be just as or more important as conductive heat flow. However, using a conductive heat flow equation will provide a first-order estimation of the regional heat flow and provide information on the regional heat flow. The one-dimensional conductive heat flow equation (Fourier's law) is

$$q = k \, dT/dz, \quad (1)$$

where  $q$  is the heat flux,  $dT/dz$  is the temperature gradient, and  $k$  is the thermal conductivity. TANAKA *et al.* (1999) showed the Curie temperature, and  $C$  can be defined as

$$C = (dT/dz)D, \quad (2)$$

where  $D$  is the CPD, provided that there are no heat sources or sinks between the earth's surface and the CPD. Then, the CPD becomes

$$D = kC/q. \quad (3)$$

An additional variable that affects the estimated heat flow is the thermal conductivity. Thermal conductivity values normally range between 1.3 and 3.3 W m<sup>-1</sup> K<sup>-1</sup> for granites to 2.5–5.0 W m<sup>-1</sup> K<sup>-1</sup> for metamorphic rocks (LILLIE 1999). TANAKA *et al.* (1999) used a range of  $kC$  (1000–2500 W m<sup>-1</sup>) to show that high flow values (>150 mW m<sup>-2</sup>) in spatially small areas (individual composite volcanoes) using the power density spectrum method cannot image local CPDs.

However, the 3D inversion results imply that local CPDs may be estimated. Using Eq. 3, CPD's between 8 and 12 km, and heat flow values between 120 and 1400 mW m<sup>-2</sup> (BLACKWELL and RICHARDS 2004), the thermal conductivities for the Salton Trough were estimated to be between 2.5 and 19.2 W m<sup>-1</sup> K<sup>-1</sup>. The high thermal conductivity values are concentrated around the Salton Sea geothermal area (Fig. 3) and do not necessarily reflect the thermal conductivities of the entire region. Using the estimated thermal conductivities and CPDs between 8 and 12 km, the estimated heat flow values within the

Salton Trough range between 133 and 1500 mW m<sup>-2</sup>. These heat flow values in general are in accord with the measured values (LACHENBRUCH *et al.* 1985; SASS *et al.* 1988, 1994) that show that the Salton Trough is a region of high heat flow (>140 mW m<sup>-2</sup>). Rapid extension, igneous intrusions, and mafic underplating within the lower crust (SASS *et al.* 1988) have been used to explain this region of high heat flow. The magnetic analysis could not image the source of the extremely high heat flows within the Salton Sea geothermal area (Fig. 3). The high values (>1200 mW m<sup>-2</sup>) are not associated with the northwest-trending magnetic maximum (central anomaly 2, Fig. 2) and are thought to be local anomalies associated with hydrothermal circulation (SASS *et al.* 1994).

If the bottom of the magnetic sources (Figs. 7, 8, 9, 10) indicates that if the bottoms of the magnetic sources are indeed the CPD, then the shallow CPDs may be related to elevated heat flow values. These values (<10 km) occur within specific regions and include the regions between the San Jacinto and Elsinore Faults, along the Brawley Fault Zone south and southwest of the Salton Sea geothermal area, southwest of the Elsinore Fault, and regions within and northeast of the Chocolate Mountains (Fig. 10). Even though the regional heat flow regime of the Salton Trough is considered to be high (SASS *et al.* 1994), the measured heat flow values do include more moderate heat flow values (50–100 mW m<sup>-2</sup>) (Fig. 3). One curious result was that the known geothermal areas (Salton Sea geothermal area and Cerro Prieto) were associated with relatively deep CPDs. Similar CPDs were found in the Cerro Prieto geothermal field (GOLDSTEIN *et al.* 1984; Fig. 1). These results imply as concluded by SASS *et al.* (1994) that these geothermal regions are related to narrow zones of hydrothermal flow, and regional magnetic analyses cannot isolate such small CPDs.

Our results suggest that the overall heat flow pattern may be more complicated because the areas of shallow CPDs are isolated regions (Fig. 10). The deeper CPD values in the southwest portions of the Imperial Valley near the Elsinore Fault coincide with higher velocities in the basement (HAN *et al.* 2013a, b). However, this region of deeper CPD values is narrow, and the region to the north and southwest and



the CPD depths are shallower. Even though the SSIP models in this region indicate higher basement velocities (HAN *et al.* 2013a, b), deeper imaging seismic ambient noise analyses indicate that below 9 km the seismic velocities are lower (BARAK *et al.* 2011). Combined with the shallow CPD values, the lower velocities may indicate that this region has some type of deep heat source related to hydrothermal processes. Deeper CPD values southeast of the Salton Sea occur in the same region as high velocities (FUIS *et al.* 1984; BARAK *et al.* 2011) caused by metamorphosed sediments with intruded by mafic material.

The region of shallow CPD values along the Brawley Fault Zone coincides with low velocities imaged by SSIP who primarily interpreted these velocities to be caused by faulting within the basement (HAN *et al.* 2013a, b). The shallow CPD values and high heat flow values (Fig. 3) imply that these low values may be partially related to high heat flow possibly caused by hydrothermal circulation or partially molten material. This zone of shallow CPDs seems to trend to the northwest along the San Jacinto Fault zone and to the southeast to the west of the Cerro Prieto geothermal field (Fig. 1). The CPD analysis alone cannot determine the source of the shallow CPD values as additional detailed seismic reflection/refraction surveys are needed to confirm the depths of these sources. Additionally, a MT survey may aid in determining if there is a partially molten body at depth.

## 6. Conclusions

The magnetic field of Salton Trough and the surrounding area was analyzed to determine the bottom of the magnetic bodies and how these relate to the regional CPD. Two methods were applied: (1) 2D power spectrum methods and (2) inversion of magnetic data for a 3D magnetic susceptibility distribution. The power spectral method determined that the CPD varied between 11 and 23 km with the deeper values being outside of the Salton Trough in the Eastern Peninsula Ranges and the Chocolate Mountains region. Within the Salton Trough, the CPD ranges from 11 to 19 km with the shallowest depths occurring in the center of the Salton Trough. The shallowest depths occur over the area where seismic

studies indicate low seismic velocities possibly related to hydrothermal circulation, fracturing in the basement, or partially molten material. The deeper values occur over regional magnetic maxima and areas with higher seismic velocities within the lower crust which may be related to basaltic material or a combination of mafic intrusions and metamorphosed sediments. Even though these values agreed with regional magnetic studies, the power spectral methods could not image small-scale variations in the CPD, as the high heat flow values under the Salton Sea geothermal area and the Cerro Prieto region imply shallow CPDs, and power spectrum results indicate deep CPDs (16 and 18 km, respectively).

The results of the 3D inversion of the magnetic data showed that the shallowest CPD depths (5–8 km) are found over the Brawley Seismic Zone and the southwest portion of the Imperial Valley near the Elsinore Fault. The shallow CPD values near the Brawley Seismic Zone may be related to hydrothermal circulation, while the shallow values near the Elsinore Fault occur over low seismic velocities between 9 and 21 km in depth that are below high velocity basement lithologies. The source of the low seismic velocities may be related to partially molten material or hydrothermal circulation. The shallow depths within the Brawley Seismic Zone also occur to the west of this zone, and this region occurs over the seismically imaged low velocity region thought to be associated with hydrothermal circulation or partially molten material. If the shallow CPD values are caused by such a geothermal system, this region extends at least 50 km to the northwest and southeast of the detailed seismic refraction profiles. To determine if magma or some type of geothermal system is present at mid-crustal levels in the Salton Trough, additional geophysical analyses including MT and seismic reflection/refraction are recommended. While the spectral and 3D inversion methods produced similar CPDs in several regions, the 3D inversion method produced higher lateral resolution of the CPD.

## Acknowledgments

We would like to thank Randy Keller for helpful discussions. We would like also to thank Carlos

Montana for technical support. Review comments by an anonymous reviewer greatly improved the paper. This work was partially supported by NSF grant number HRD-0734825.

## REFERENCES

- ALLAM, A., and BEN-ZION, Y. (2012) *Seismic velocity structures in the southern California plateboundary environment from double-difference tomography*. *Geophysical Journal International* 190, 1181–1196.
- ATWATER, T. (1970), *Implications of plate tectonics for the Cenozoic evolution of western North America*, Geological Society of America Bulletin 81, 3513–3536.
- AXEN, G., and FLETCHER, J. (1998), *Late Micoene-Pliocene extensional faulting, northern Gulf of California, Mexico, and Salton Trough, California*, *International Geology Review* 40, 219–244.
- AXEN, G., GROVE, M., STOCKLI, D., LOVERA, O., ROTHSTEIN, D., FLETCHER, J., FARLEY, K., and ABBOTT, P. (2000), *Thermal evolution of Monte Blanco dome: Low-angle normal faulting during Gulf of California rifting and late Eocene denudation of the eastern Peninsular Ranges*, *Tectonics* 19, 197–212.
- BANKEY, V., CUEVAS, A., DANIELS, D., FINN, C., HERNANDEZ, I., HILL, P., KUCKS, R., MILES, W., PILKINGTON, M., ROBERTS, C., ROEST, W., RYSTROM, V., SHEARER, S., SNYDER, S., SWEENEY, R., VELEZ, J., PHILLIPS, J., and RAVAT, D. (2002), *Digital data grids for the magnetic anomaly map of North America*, U.S. Geological Survey Open-File Report 02-414, US Geological Survey, Denver, Colorado, USA.
- BARAK, S., KLEMPERER, S., LAWRENCE, J., and CASTRO, R. (2011), *Passive seismic study of a magma dominated rift: the Salton Trough*, Abstract T33G-2496 presented at 2011 Fall Meeting of American Geophysical Union.
- BARANOV, V. (1957), *A new method for interpretation of aeromagnetic maps: Pseudogravimetric anomalies*, *Geophysics* 22, 359–383.
- BHATTACHARYYA, B., and LEU, L. (1975), *Spectral analysis of gravity and magnetic anomalies due to two dimensional structures*, *Geophysics* 40, 993–1013.
- BIEHLER, S. (1964), *Geophysical study of the Salton Trough of southern California*, Ph.D. Thesis (Caltech Institute of Technology, Pasadena, CA.).
- BLACKWELL, D., and RICHARDS, M. (2004), *Calibration of the AAPG geothermal survey of North America BHT database*. American Association of Petroleum Geologists. Annual Meeting, paper 87616, Dallas, TX.
- BLAKELY, R. (1988), *Curie temperature isotherm analysis and tectonic implications of aeromagnetic data from Nevada*, *Journal of Geophysical Research* 93, 11817–11832.
- BOULIGAND, C., GLEN, J., and BLAKELY, R. (2009), *Mapping Curie temperature depth in the western United States with a fractal model for crustal magnetization*, *Journal of Geophysical Research* 114. doi:10.1029/2009JB006494.
- BROTHERS, D., DRISCOLL, N., KENT, G., HARDING, A., BABCOCK, J., and BASKIN, R. (2009), *Tectonic evolution of the Salton Sea inferred from seismic reflection data*, *Nature Geoscience*. doi:10.1038/N GEO590.
- BYERLY, P. E., and STOLT, R. H. (1977), *An attempt to define the Curie point isotherm in Northern and Central Arizona*, *Geophysics* 42, 1394–1400.
- CHAPMAN, D., and FURLONG, K. (1992), *The thermal state of the lower crust*, In: FOUNTAIN, D., ARCULUS, R., and KAY, R., (Eds.), *Continental Lower Crust, Developments in Geotectonics*, Elsevier, pp. 179–199.
- DE BOER, J. (1980), *Paleomagnetism of the Quaternary Cerro Prieto, Crater Elegante, and Salton Buttes volcanic domes in the northern part of the Gulf of California rhombochasm* Proceedings of the Second Symposium on the Cerro Prieto Geothermal Field, Baja California, Mexico. p. 1–8.
- DEMETS, C., and DIXON, T. (1999), *New kinematic models for Pacific-North America motion from 3 Ma to present: 1. Evidence for steady motion and biases in the NUVEL-1A model*. *Results, Geophysical Research Letters* 26, 1921–1924.
- DORSEY, R. (2010), *Sedimentation and crustal recycling along an active oblique-rift margin: Salton Trough and northern Gulf of California*, *Geology* 38, 443–446.
- DORSEY, R., FLUETTE, A., MCDUGALL, K., HOUSEN B., JANECKE, S., AXEN, G., and SHIRVELL, C. (2007), *Chronology of Miocene-Pliocene deposits at Split Mountain Gorge, southern California: A record of regional tectonics and Colorado River evolution*, *Geology* 35, 57–60.
- DORSEY, R., and UMHOEFER, P. (2012), *Influence of sediment input and plate-motion obliquity on basin development along an active oblique-divergent plate boundary: Gulf of California and Salton Trough*. In: BUSBY, C., AZOR, A. (Eds.), *Tectonics of Sedimentary Basins: Recent Advances*, Blackwell Publ., pp. 209–225.
- DOSER, D., and KANAMORI, H. (1986), *Depth of seismicity in the Imperial Valley Region (1977–1983) and its relationship to heat flow, crustal structure and the October 15, 1979, earthquake*. *Journal of Geophysical Research* 91, 675–688.
- ELDER, W., REX, R., MALDAY, T., ROBINSON, P., and BIEHLER, S. (1972), *Crustal spreading in southern California*, *Science* 178, 15–24.
- ESPINOSA-CARDENA, J., and CAMPOS-ENRIQUEZ, J. (2008), *Curie point depth from spectral analysis of aeromagnetic data from Cerro Prieto geothermal area, Baja California, Mexico*. *Journal of Volcanology and Geothermal Research* 176, 601–609.
- FAY, N., HUMPHREYS, E. (2005), *Fault slip rates, effects of elastic heterogeneity on geodetic data and the strength of the lower crust in the Salton Trough region, southern California*, *Journal of Geophysical Research* 110, B09401. doi:10.1029/2004JB003548.
- FIALKO, Y. (2006), *Interseismic strain accumulation and the earthquake potential on the southern San Andreas fault system*, *Nature* 441, 968–971.
- FUIS, G., MOONEY, W., HEALY, J., McMECHAN, G., and LUTTER, W. (1984), *A seismic refraction survey of the Imperial Valley Region, California*. *Journal of Geophysical Research* 89, 1165–1189.
- GOLDSTEIN, N., WILT, M., and CORRIGAN, D. (1984), *Analysis of the Nuevo Leon magnetic anomaly and its possible relation to the Cerro Prieto magmatic-hydrothermal system*, *Geothermics* 13, 3–11.
- GRISCOM, A., and JACHENS, R. (1990), *Crustal and lithospheric structure from gravity and magnetic studies*. In: WALLACE, R. (Ed.), *The San Andreas Fault System*, U. S. Geological Survey Professional Paper 1515, 239–259.

- GRISCOM, A., MUFFLER, L. (1971), *Aeromagnetic map and interpretation of the Salton Sea geothermal area, California*. U.S. Geological Survey. Geophysical Investigation Map GP-754.
- HAGGERTY, S.E. (1978), *Mineralogical constraints on Curie isotherms in deep crustal-magnetic boundaries*, Geophysical Research Letters 5, 105–108.
- HAN, L., HOLE, J., STOCK, J., FUIS, G., RYMER, M., DRISCOLL, N., KENT, G., HARDING, A., GONZALEZ-FERNADEZ, A., and LAZARO-MANCILLA, O. (2013), *The Salton Seismic Imaging Project (SSIP): Active rift process in the Brawley Seismic Zone*, American Geophysical Union Fall Meeting Abstract T33G-2498.
- HAN, L., HOLE, J., DELPH, J., LIVERS, A., WHITE-GAYNOR, A., STOCK, J., FUIS, G., DRISCOLL, N., KELL, A., and KENT, G. (2013), *Crustal structure during active continental rifting in Central Salton Trough, California, constrained by The Salton Seismic Imaging Project (SSIP)*: Geological Society of America Program with Abstracts, 44, 305.
- HERZIG, C., and JACOBS, D. (1994), *Cenozoic volcanism and two-stage extension in the Salton Trough, southern California and northern Baja California*, Geology 22, 991–994.
- HONG, M. R. (1982), *The inversion of magnetic and gravity anomalies and the depth to Curie isotherm*, Ph.D. Thesis (University of Texas at Dallas, Richardson, Tx. USA).
- HUSSEIN, M., MICKUS, K., and SERPA, L. (2012), *Curie point depth estimates from aeromagnetic data from Death Valley and surrounding regions, California*. Pure and Applied Geophysics 170, 617–632.
- HUSSEIN, M., VELASCO, A., and SERPA, L. (2011), *Crustal structure of the Salton Trough: Incorporation of receiver function, gravity and magnetic data*, International Journal of Geosciences 2, 502–512.
- JENNING, C. (1977), *Geological map of California*, Sacramento, California. California Division of Mines and Geology. Scale 1:750,000.
- KINSELLA, A., BARAK, S., and KLEMPERER, S. (2012), *Rapid lateral variation of seismic anisotropy across the Salton Trough, California*, Abstract T51B-2576 presented at 2011 Fall Meeting of American Geophysical Union.
- KOHLER, W., and FUIS, G. (1986), *Travel time, time-term, and basement depth maps for Imperial Valley region, California from explosion*, Bulletin Seismological Society of America 79, 1289–1303.
- LACHENBRUCH, A., SASS, J., and GALANIS, S. (1985), *Heat flow in southernmost California and the origin of the Salton Trough*, Journal of Geophysical Research 90, 6709–6736.
- LANGENHEIM, V., and JACHENS, R. (2003), *Crustal structure of the Peninsula Ranges batholiths from magnetic data: Implications for Gulf of California rifting*. Geophysical Research Letters 30, 1597, doi:10.1029/2003GL017159.
- LANGENHEIM, V., JACHENS, R., MATTI, J., HAUSSON, E., MORTON, D., and CHRISTENSEN, A. (2005), *Geophysical evidence for wedging in the San Geronio Pass structural knot, southern, San Andreas fault zone, southern California*, Geological Society of America Bulletin 117, 1554–1572.
- LANGENHEIM, V., JACHENS, R., MORTON, D., KISTLER, R., and MATTI, J. (2004), *Geophysical and isotopic mapping of preexisting crustal structures that influenced the location and development of the San Jacinto fault zone, southern California*, Geological Society of America Bulletin 116, 1143–1157.
- LANGENHEIM, V., and POWELL, R. (2009), *Basin geometry and cumulative offsets in the Eastern Transverse Ranges, southern California: Implications for transrotational deformation along the San Andreas fault system*, Geosphere 5, 1–22.
- LEWIS, J., DAY, S., MAGISTRALE, H., EAKINS, J., and VERNON, F. (2000), *Regional crustal thickness variations of the Peninsular Range, southern California*, Geology 28, 303–306.
- LI, Y., and OLDENBURG D.W. (1996), *3D inversion of magnetic data*, Geophysics 61, 394–408.
- LILLIE, R.J. (1999), *Whole Earth Geophysics—An Introductory Textbook for Geologists and Geophysicists*. Prentice Hall Publishing, pp 239.
- LINDSEY, E., SAHAKIAN, V., FIALKO Y., BOCK Y., BARBOT S., and ROCKWELL T. (2013), *Interseismic strain localization in the San Jacinto Fault Zone*, Pure and Applied Geophysics 171, 1–18.
- MANEA, M., and MANEA, V. (2011), *Curie point depth estimates and correlation with subduction in Mexico*, Pure and Applied Geophysics 168, 1489–1499.
- MAUS, S., and DIMRI, V. (1996), *Depth estimation from the scaling power spectrum of potential fields*, Geophysical Journal International, 124, 113–120.
- MAUS, S., GORDON, D., and FAIRHEAD, D. (1997), *Curie temperature depth estimation using a self similar magnetization model*, Geophysical Journal International 129, 163–168.
- MICKUS, K. (1989), *Backus and Gilbert inversion of two and one-half dimensional gravity and magnetic anomalies and crustal structure studies in western Arizona and the eastern Mojave Desert, California*, Ph.D. Thesis (University of Texas at El Paso, El Paso, TX, USA).
- MICKUS, K., and JAMES, C. (1991), *Regional gravity studies in southeastern California, western Arizona, and southern Nevada*, Journal of Geophysical Research 96, 12,333–12,350.
- MORAN-ZENTENO, D., WILSON, J., and SANCHEZ-BARRERA, L. (1994), *The Geology of the Mexican Republic*. American Association of Petroleum Geologists Studies in Geology 39, 160 pp.
- NEWMARK, R., KASAMEYER, P., and YOUNKER, L. (1988), *Shallow drilling in the Salton Sea Region: The thermal anomaly*, Journal of Geophysical Research 93, 13,005–13,023.
- OKUBO, Y., GRAF, R., HANSEN, R., OGAWA, K., and TSU, H. (1985), *Curie depths of the island of Kyushu and surrounding areas, Japan*, Geophysics 53, 481–494.
- OSKIN, M., STOCK, J., and MARTÍN-BARAJÁS, A. (2001), *Rapid localization of Pacific–North America plate motion in the Gulf of California*, Geology 29, 459–462.
- PARSONS, T., and MCCARTHY, J. (1996), *Crustal and upper mantle velocity structure of the Salton Trough, southeast California*, Tectonics 15, 456–471.
- POLLACK, H., HURTER, S., and JOHNSON, J. (1993), *Heat flow from the Earth's interior: Analysis of the global data set*, Reviews of Geophysics 31, 267–280.
- RAVAT, D., PIGNATELLI, A., NICOLOSI, I., and CHIAPPINI, M. (2007), *A study of spectral methods of estimating the depth to the bottom of magnetic sources from near-surface magnetic anomaly data*, Geophysical Journal International 169, 421–434.
- ROSS, H., BLAKELY, R., and ZOBACK, M. (2006), *Testing the use of aeromagnetic data for the determination of Curie depth in California*, Geophysics 71, L51–L59. doi:10.1190/1.2335572.
- SANDERS, C., and MAGISTRALE, H. (1997), *Segmentation of the northern San Jacinto fault zone, southern California*, Journal of Geophysical Research, 102, 27,453–27,467.
- SANO, Y., and WAKITA, H. (1985), *Geographical distribution of <sup>3</sup>He/<sup>4</sup>He ratios in Japan: Implications for arc Tectonics and*

- incipient magmatism*, *Journal of Geophysical Research* 90, 8729–8741.
- SASS, J. H., LACHENBRUCH, A. H., GALANIS, S. P., MORGAN, P., PRIEST, S. S., MOSES, T. H., and MUNROE, R. J. (1994), *Thermal regime of the southern Basin and Range province: 1. Heat flow data from Arizona and the Mojave Desert of California and Nevada*, *Journal of Geophysical Research* 99, 22,093–22,119.
- SASS, J., PRIEST, S., DUDA, L., CARSON, C., HENDRICKS, J., and ROBISON, L. (1988), *Thermal regime of the state 2–14 well, Salton Sea scientific drilling project*, *Journal of Geophysical Research* 93, 12,995–13004.
- SCHMITT, A. and VAZQUEZ, J. (2006), *Alteration and remelting of nascent oceanic crust during continental rupture: Evidence from zircon geochemistry of rhyolites and xenoliths from the Salton Trough, California*, *Earth and Planetary Science Letters* 252, 260–272.
- SHUEY, R., SCHELLINGER, D., TRIPP, A., and ALLEY, L. (1977), *Curie depth determination from aeromagnetic spectra*, *Geophysical Journal of the Royal Astronomical Society* 50, 75–101.
- SPECTOR, A., and GRANT, F. (1970), *Statistical models for interpreting aeromagnetic data*, *Geophysics* 35, 293–302.
- STEELY, A., JANECKE, S., DORSEY, R., and AXEN, G. (2009), *Early Pleistocene initiation of the San Felipe fault zone, SW Salton Trough, during reorganization of the San Andreas fault system*, *Geological Society of America Bulletin* 121, 663–687.
- SWANBERG, C., and MORGAN, P. (1978), *The linear relation between temperatures based on silica content of groundwater and regional heat flow: A new heat flow map of the United States*, *Pure and Applied Geophysics* 117, 227–241.
- TANAKA, A., OKUBO, Y., and MATSUBAYASHI, O. (1999), *CPD based on spectrum analysis of the magnetic anomaly data in East and Southeast Asia*, *Tectonophysics* 306, 461–470.
- WESNOSKY, S., 1986, *Earthquakes, Quaternary faults, and seismic hazard in California*, *Journal of Geophysical Research*, 91, 12,587–12,631.
- YANG, Y., and FORSYTH, D. (2008), *Attenuation in the upper beneath Southern California: Physical state of the lithosphere and asthenosphere*, *Journal of Geophysical Research* 113, B03308. doi:[10.1029/2007/JB005118](https://doi.org/10.1029/2007/JB005118).
- ZHU, L., and KANAMORI, H. (2000), *Moho depth variation in southern California from teleseismic receiver functions*, *Journal of Geophysical Research* 105, 2969–2980.

(Received September 8, 2014, revised April 24, 2015, accepted May 4, 2015, Published online May 19, 2015)